



Experimental investigation in controlled conditions of the impact of dynamic spectrum sharing on maximum-power extrapolation techniques for the assessment of human exposure to electromagnetic fields generated by 5G gNodeB

Sara Adda¹, Tommaso Aureli², Tiziana Cassano³, Daniele Franci², Marco D. Migliore⁴, Nicola Pasquino⁵, Settimio Pavoncello², Fulvio Schettino⁴, Maddalena Schirone³

¹ ARPA Piemonte, Dipartimento Rischi Fisici e Tecnologici, Via Jervis 30, 10015 Ivrea (TO), Italy

² ARPA Lazio, 00172 Rome, Italy

³ ARPA Puglia, UOS Agenti Fisici, DAP Bari, Corso Trieste 27, 70126 Bari, Italy

⁴ Dipartimento di Ingegneria Elettrica e dell'Informazione (DIEI) "Maurizio Scarano", University of Cassino and Southern Lazio, Cassino, 03043, and CNIT Cassino, and Eledia@UNICas, Italy

⁵ Dipartimento di Ingegneria Elettrica e delle Tecnologie dell'Informazione (DIETI), Università degli Studi di Napoli Federico II, 80125 Napoli, Italy

ABSTRACT

Maximum-Power Extrapolation (MPE) techniques adopted for 4G and 5G signals are applied to systems using Dynamic Spectrum Sharing (DSS) signals generated by a base station and transferred to the measurement instruments through an air interface adapter to obtain a controlled environment. This allowed to focus the analysis on the effect of the frame structure on the MPE procedure, excluding the random effects associated to fading phenomena affecting signals received in real environments. The analysis confirms that both the 4G MPE and the proposed 5G MPE procedure can be used for DSS signals, provided that the correct number of subcarriers in the DSS frame is considered.

Section: RESEARCH PAPER

Keywords: Dynamic spectrum sharing; maximum-power extrapolation; DSS; 4G; 5G; human exposure; measurements

Citation: Sara Adda, Tommaso Aureli, Tiziana Cassano, Daniele Franci, Marco D. Migliore, Nicola Pasquino, Settimio Pavoncello, Fulvio Schettino, Maddalena Schirone, Experimental investigation in controlled conditions of the impact of dynamic spectrum sharing on maximum-power extrapolation techniques for the assessment of human exposure to electromagnetic fields generated by 5G gNodeB, Acta IMEKO, vol. 11, no. 3, article 18, September 2022, identifier: IMEKO-ACTA-11 (2022)-03-18

Section Editor: Francesco Lamonaca, University of Calabria, Italy

Received March 17, 2022; **In final form** September 15, 2022; **Published** September 2022

Copyright: This is an open-access article distributed under the terms of the Creative Commons Attribution 3.0 License, which permits unrestricted use, distribution, and reproduction in any medium, provided the original author and source are credited.

Corresponding author: Nicola Pasquino, e-mail: nicola.pasquino@unina.it

1. INTRODUCTION

Dynamic Spectrum Sharing (DSS) is becoming a key technology in the implementation of 5G networks thanks to several practical advantages. DSS provides 5G services on 4G Long Term Evolution (LTE) networks, thus allowing to use the 4G facilities for a quick deployment of 5G networks without the need of new frequency bands, not always available to local operators. Consequently, it is a simple solution that requires basically only software updates, allowing operators to start nationwide 5G coverage with limited costs. Furthermore, the use

of 4G frequency bands allows better area coverage and indoor penetration compared to sub-6 GHz and Frequency Range 2 (FR2) (24.25 GHz to 52.6 GHz) used in both Non-Standalone (NSA) and Standalone (SA) 5G networks. In this paper, an experimental investigation is presented to evaluate if this technological solution impacts the outcomes of measurement techniques used to assess the compliance with electromagnetic fields (EMF) exposure limits.

Maximum-Power Extrapolation (MPE) measurement has been object of a consolidated literature, and standards for MPE measurements are available [1]. 5G is a more recent technology, however, although standards are still under development, MPE

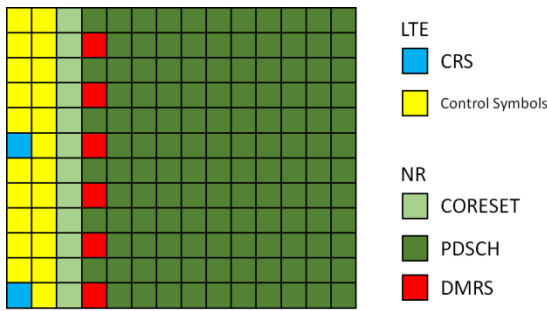


Figure 1. An example of LTE/NR subframe; the first two time slots are always reserved to LTE.

procedures have been described in a few research papers [2]-[6]. 5G DSS is midstream between 4G and 5G technology. In this paper MPE techniques adopted for 4G signals and 5G signals are applied to DSS signals. In particular, the DSS signals generated by an actual base station have been connected to the measurement equipment through an Air Interface Adapter (AIAD). This allows to focus the analysis on the effect of the frame structure on the MPE procedure, excluding the random effects due to fading phenomena affecting signals received in real environments. The results confirm that both 4G and 5G MPE extrapolation techniques allow a correct estimation of the MPE level of DSS signals, provided that the correct number of the subcarriers in the DSS frame is considered.

2. THE DYNAMIC SPECTRUM SHARING TECHNIQUE

As noted in the Introduction, Spectrum Sharing (SS) allows network operators to implement 5G NR using existing LTE frequency bands, with relatively inexpensive software upgrades. There are two possible solutions to LTE-NR coexistence: Static Spectrum Sharing (SSS), where the frequency band is statically assigned to either system over time, and DSS, where resources are switched between LTE and 5G dynamically over time. SSS is less attracting than DSS, particularly in the current state of 5G implementation, where penetration of 5G devices is still limited and most traffic is on LTE, providing an almost fully loaded 4G carrier and an almost empty 5G carrier. This strongly pushes towards the implementation of DSS which allows LTE and 5G NR to share spectrum resources dynamically based on the current traffic demand, thus employing the entire available bandwidth more efficiently. Accordingly, the solution currently adopted in Italy is DSS. DSS supports 5G numerology with $\mu = 0$

(15 kHz subcarrier spacing) and $\mu = 1$ (30 kHz spacing). Although, as will be briefly discussed below, implementation of $\mu = 1$ numerology in a 4G frame is less complex than the use of $\mu = 0$, in this Section we will focus our attention on the DSS technology with $\mu = 0$ download frame structure, since it is the same adopted in the signals used in the presented experimental activity.

To avoid imperfect signal synchronization, in case of LTE-NR coexistence, it is crucial to avoid overlapping between NR Synchronization Signal Block (SSB) and LTE Reference Signal (CRS).

Let us consider the LTE frame. The CRS is transmitted in 4 (using 1 or 2 antenna ports) or 6 (when using 4 antenna ports) non-contiguous OFDM symbols of each subframe. With respect to NR, SSB requires four consecutive OFDM symbols. In case of $\mu = 1$, two NR Resource Elements (REs) occupy the duration of an LTE RE (whose spacing is 15 kHz). Consequently, an SSB only occupies two LTE symbols. This makes it possible to insert the SSBs in the LTE frame in a simple way, since in the LTE frame the distance between two consecutive CRS is greater than the duration of two LTE OFDM symbols in case of any number of antenna ports.

Things become more involved when a 5G signal with $\mu = 0$ numerology must be inserted in an LTE frame. In fact, as noted above, there are only 3 contiguous OFDM symbols without any CRS transmissions, while SSB requires 4 symbols with 15 kHz subcarrier spacing.

The solution currently applied involves the use of 4G Multimedia Broadcast multicast service Single Frequency Network (MBSFN) subframes. MBSFN has been introduced in the LTE standard as part of release 9 for point-to-multipoint communication to provide broadcast and multicast services (evolved Multimedia Broadcast Multicast Services (eMBMS)). The network can configure six out of ten subframes forming the LTE radio frame to become MBSFN subframes. Based on the 3GPP standard, these could be subframes #1, #2, #3, #6, #7, and #8 of a radio frame. A standard LTE terminal reads in the MBSFN configuration from system information in block Type 2 (SIB2) and ignores the subframes configured for broadcast. To allow effective broadcasting transmission, the MBSFN subframes reserve only the first 2 OFDM symbols to carry the control channels for LTE, while the remaining ones are reserved for eMBMS (Figure 1). These symbols are consequently "free".

To better explain this point, that is important for the MPE procedure, in Figure 2 an example of a DSS frame structure (right) is qualitatively compared with the spectrum of the DSS

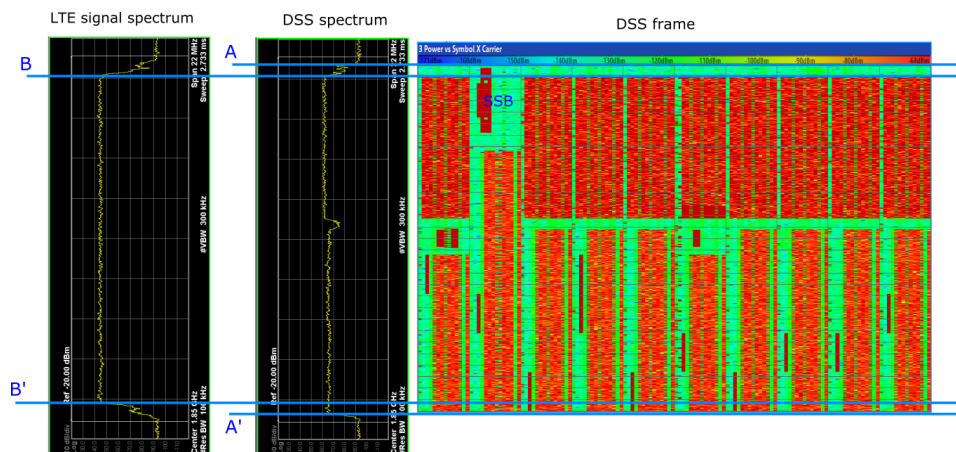


Figure 2. Qualitative relationship between the spectrum of the LTE signal, the spectrum of the DSS signal and the DSS frame.



Figure 3. Experimental setup used throughout the measurement campaign.

signal (centre). Furthermore, the spectrum of a legacy 4G signal (i.e., without DSS) is shown in the left. Regarding the DSS frame structure, we can note an MBSFN in the second subframe, where the SSB of the 5G signal is placed. The 4G signal uses the upper half part of the remaining subframes, while the 5G signal uses the lower half part of these subframes, and the part not used by the SSB of the MBSF subframe. Note that 5G does not use the first two symbol of the frames, that are reserved to 4G. The spectrum of the DSS is shown in the centre figure. The useful spectrum is in the A-A' frequency range. The left plot shows an example of a standard 4G spectrum. Due to the presence of a larger band-guard, the useful portion of the spectrum is limited to the B-B' frequency range, obtaining a lower number of subcarriers.

In practice, although both 4G and 5G standard signals occupy a nominal bandwidth of 20 MHz, the actual useful bandwidth for a 5G signal is 1.08 MHz larger than the corresponding 4G bandwidth, i.e., 19.08 vs 18 MHz. Accordingly, the number of subcarriers of a 20 MHz nominal-bandwidth DSS signal is 1272. All of them are available for 5G signals, while only 1200 are used for LTE signals.

3. MAXIMUM-POWER EXTRAPOLATION TECHNIQUE FOR 4G AND 5G SIGNALS

The final goal of the MPE procedure is the estimation of the maximum field level E^{max} that could be reached in the measurement point [1]. This quantity is used as a reference to estimate the EMF exposure in realistic conditions by a suitable scaling factor [1], [7]-[15].

Both 4G and 5G use OFDMA. This gives many similarities that can be exploited for the MPE of DSS signals. More specifically, they require [1], [16]:

- a. Information on the structure of the frame (as bandwidth, numerology for 5G, duty cycle in case of TDD transmissions) necessary to identify the number of REs available for downlink transmission,
- b. the estimation of E_{RE}^{max} , the maximum possible average EMF level associated to a RE.

In 4G, E_{RE}^{max} can be obtained considering the power of the REs associated to the Reference Signal (RS) of the 4G frame, let E_{RS} be, that are transmitted at full power. According to [1], the maximum EMF level in the measurement location is then estimated as

$$E_{4G}^{max} = E_{RS} \sqrt{\frac{N_{sc} F_{TDC}}{F_B}}, \quad (1)$$

where N_{sc} is the total number of subcarriers, F_{TDC} is a duty cycle factor that describes the transmission scheme implemented by

the signal, F_B is a boosting factor that can be applied to the 4G control channels transmitted power to extend the coverage range.

In 5G NR, the only signal that is always 'on air' is the SSB, that is transmitted at constant and maximum power. It must be noted that in NR it is possible to use different beams to transmit SSB (using broadcast beams) and payload data (using traffic beams). Accordingly, measurement of the power of the REs of the SSB in general does not allow a direct estimation of E_{5G}^{max} , that is related to the traffic beams [5]. However, as discussed in the previous Section, DSS usually is obtained by only software upgrading of the 4G system. Consequently, SSB and payload data are transmitted on the same beam. This allows to estimate E_{5G}^{max} directly from the measurement of SSB REs power. Following the experimental approach discussed in [17], the power of the REs associated to the Physical Broadcast Channel DeModulation Reference Signal (PBCH-DMRS) is used as input for the extrapolation formula:

$$E_{5G}^{max} = E_{PBCH_DMRS} \sqrt{N_{sc} F_{TDC} F_{beam}}, \quad (2)$$

where F_{beam} is a correction factor that considers the difference between traffic and broadcast beams gain. It's worth noticing that for DSS signals generated by passive MIMO systems like the one used in our experiment, $F_{beam} = 1$ since SSB and traffic data share the same beam.

4. EXPERIMENTAL RESULTS

An experimental session has been carried out in a dedicated facility, used by one of the main Italian telco companies for test purposes. Measurements were performed with the aim of gaining a suitable understanding of DSS system operation and thus defining an effective procedure for the assessment of the population exposure from DSS sources. The experimental setup used during this controlled-environment experimental session is described in the following:

- a Keysight MXA N9020A Vector Signal Analyzer (VSA) with up to 20 MHz demodulation bandwidth, equipped with demodulation software for both 4G and 5G NR signals;
- a Rhode & Schwarz FSVA3044 VSA with up to 400 MHz demodulation bandwidth, equipped with demodulation software for both 4G and 5G NR signals.

The experimental setup is shown in Figure 3. To ensure a reliable emulation of both inputs and outputs according to the demands of real users, the signal generated by the base station has been transferred to an AIAD 8/8-4G+DL manufactured by MTS Systemtechnik. The aim of the AIAD is to emulate the air interface, allowing for testing of mobile radio base stations in a laboratory. Figure 4 shows the AIAD frontend with two coaxial cables used to transfer both MIMO branches of the DSS signal from the lower levels of the gNodeB to the antennas placed inside the AIAD chamber. The coaxial cable on the left of the figure is used to drive the test signal to the measurement instruments. The main characteristics of the generated signals are summarized in Table 1.

To investigate 4G-5G sharing mechanism properly, different data traffic scenarios have been considered:

- zero-traffic,
- full-frame 4G-only traffic,
- full-frame mixed 4G-5G traffic.



Figure 4. The AIAD used to transfer the signal from the base station to the measurement equipment.

Table 1. CAPTION DSS Signal Configuration

Center frequency f_c	1850 MHz
Bandwidth B	20 MHz
Duplexing	FFD
Numerology μ	0
Sub-carrier spacing Δf	15 kHz
Cell Identity (CID)	255
MIMO antennas	2
MBSFN subframe indexes	1, 21, 22
SSB allocation	Case A with $L_{max} = 4$
SSB center frequency f_{ssb}	1857,65 MHz
SSB per burst	1
SSB transmission periodicity	20 ms

4.1. Zero-traffic scenario

As a first step, a DSS signal with no data traffic was generated. Figure 5 shows the map of the demodulated power vs. symbol/carrier for an entire 10 ms DSS frame, made of ten consecutive subframes. The absence of user data traffic allows for an easy identification of both LTE and NR control channels:

- LTE Primary and Secondary Synchronization Signals (PSS and SSS) and PBCH are transmitted in subframes 0 (PSS+SSS+PBCH) and 5 (PSS+SSS only); these signals occupy about 1MHz at the centre of the signal bandwidth. In addition, the RS is located sparsely throughout the frame, according to the positions defined by 3GPP standard [18];
- 5G NR Synchronization Signal Block (SSB) can be recognized in the MBSFN subframe 1, with a frequency offset of 7.65 MHz with respect to the centre of the signal bandwidth. According to $\mu = 0$ numerology, the SSB bandwidth is equal to 3.6 MHz.

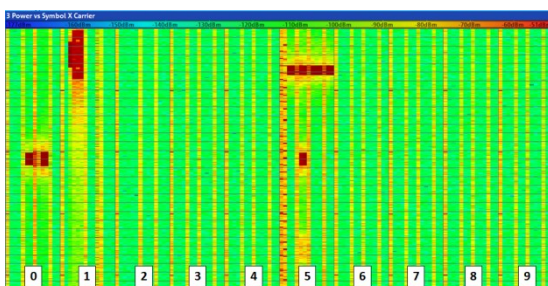


Figure 5. Power vs. symbol \times carrier map of a DSS frame in case of absence of user data traffic.

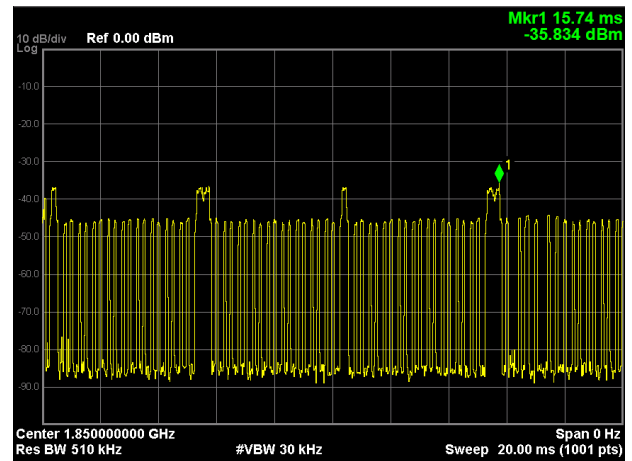


Figure 6. Zero span measurement at 1850 MHz.

Obviously, the peculiar allocation of the radio resources in DSS systems is specifically designed with the aim of avoiding any possible interference between different signals. Zero-span measurement is an alternative experimental approach useful to appreciate the resource allocation adopted by DSS. It provides the time-domain variation of the received power at a fixed frequency value. This method has the great advantage of providing a low-cost alternative to usage of top-notch, high expensive Vector Signal Analysers VSAs, since it can be accomplished by almost every traditional spectrum analyser. Figure 6 and Figure 7 show a 20-ms zero-span acquisition at 1850 MHz (i.e., the centre of the signal bandwidth) and 1857.65 MHz (i.e., SSB centre frequency) respectively. A periodic trigger equal to the frame duration (i.e., 10 ms) has been applied to both the acquired spectra.

When 1850 MHz is imposed as central frequency, the LTE control channels can be easily recognized in the acquired spectrum (Figure 6) as power bursts, spaced out 5 ms apart. Otherwise, when the central frequency is shifted to 1857.65 MHz (Figure 7), we can distinguish a unique power peak, corresponding to the 5G SSB. It is worth noting that LTE RS are present everywhere throughout the time frame, regardless of the centre frequency chosen for the measurement. The DSS signal was properly demodulated by both 4G and 5G analysis software, with both the routines characterized by an excellent synchronization with the DSS signal and reconstructed IQ constellations very close to the ideal ones.

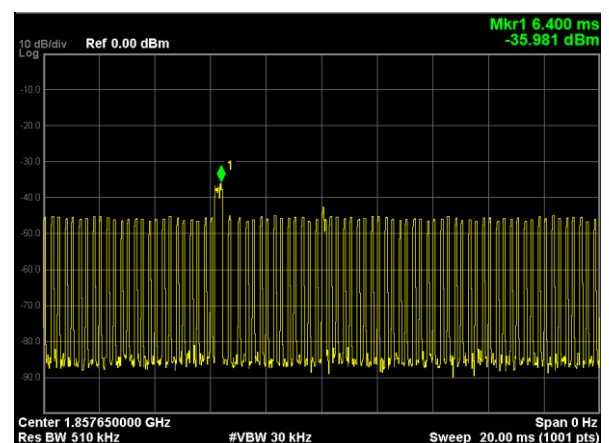


Figure 7. Zero span measurement at 1857.65 MHz.

4.2. Full-frame traffic scenario

Full-frame data traffic scenario has been achieved using a User Equipment (UE) in combination with the AIAD system, with the aim of forcing the saturation of the DSS frame through multi-thread FTP connections. To understand which schedule is used by the DSS system for resource allocation, two different scenarios have been considered:

- 100 % 4G data traffic;
- 50 % 4G – 50 % 5G data traffic.

Following the approach used in the previous section, the map of the demodulated power vs. symbol/carrier has been acquired for both scenarios under investigation. Note that to appreciate the periodicity of the MBSFN subframes, the capture buffer has been extended to 4 radio frames (i.e., 40 ms).

In absence of 5G users, and with heavy 4G traffic, all the subframes of a frame, except those configured as MBSFN, are used for 4G communication, as shown in Figure 8. In fact, MBSFN subframes (indexed as 1, 21 and 22) are not allowed to host 4G data transmission and, for this reason, they are left almost completely empty, except for 5G SSBs, which are located at the very top edge of DSS spectrum and transmitted once per couple of frames (20 ms). The presence of MBSFN subframes which are reserved for 5G transmission implies that a DSS frame cannot be entirely filled by 4G data traffic only.

Figure 9 shows the case of large 4G and 5G data traffic. 4G data is placed in upper half- part of the no-MBSFN subframes, while 5G uses most of the lower part. As discussed in Section 2, the configuration of the 5G part of frame leaves free the REs required for 4G signalling, making the presence of 5G REs completely transparent for a 4G user.

Note that the radio resource occupation is now more uniform than the previous case, although several blank regions – acting as guard intervals to avoid possible interferences between signals – are disseminated throughout the whole radio frame.

4.3. MPE procedure applied to DSS

The above-described code-domain analysis provides direct information on the following two quantities required for extrapolation procedures:

- RS for 4G (P_{RS}),
- PBCH-DMRS for 5G ($P_{PBCH-DMRS}$).

To discuss the DSS MPE procedure, we consider the full-frame condition configuration. This makes it possible to compare the results with the maximum reference power obtained by a Channel Power (CP) measurement acquired in the full-frame data traffic scenario.

As discussed in the previous section, both 4G and 5G control channel coexist within the DSS frame. For this reason, both 4G and 5G MPE procedure – described by Eq. (3) and (4) respectively – can be applied:

$$P_{4G}^{\max} = \frac{N_{sc} F_{TDC}}{F_B} P_{RS} \quad (3)$$

$$P_{5G}^{\max} = N_{SC} F_{beam} F_{TDC} P_{PBCH-DMRS} \quad (4)$$

Note that Eq. (3) and (4) represent the same MPE procedures described by Eq. (1) and (2), just applied in terms of maximum power instead of electric field. Regarding the measurement procedure, it is the same described in [1] for 4G and in [17] for 5G. More specifically, code domain measurement of the DSS signal provides direct information on PRS and $P_{PBCH-DMRS}$. According to the characteristic of the DSS signal, several

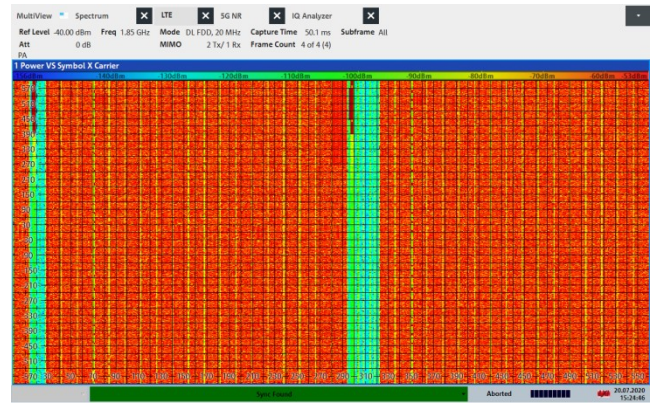


Figure 8. Power vs. symbol \times Carrier map of a DSS frame in case of 4G full traffic case; the 20 ms periodicity of the SSB is visible.

assumptions about the parameters included in Eq. (3) and Eq. (4) can be made:

- F_{TDC} is assumed to be equal to 1 in both Eq. (3) and (4), since the DSS signal adopts the Frequency Division Duplexing (FDD) transmission mode. FDD allows uplink and downlink transmission over different frequency bands, so that no uplink-downlink time duty cycle is needed,
- $F_B = 1$ in Eq. (3), since no power boost is applied to 4G RS,
- $F_{beam} = 1$ in Eq. (4), since the passive antennas used for DSS signals are not allowed for beamforming.

Regarding the N_{SC} value, as pointed out in Sect. 2, although 4G and 5G standard signals occupy a nominal bandwidth of 20 MHz, the actual occupied bandwidth of a 5G signal is 1.08 MHz larger than the corresponding 4G bandwidth (i.e., 19.08 MHz vs. 18 MHz), giving 1272 available subcarriers spaced by 15 kHz. Therefore, the value of N_{SC} is assumed to be equal to 1272 in both Eq. (3) and (4).

When a subframe transmits 4G signals only, just 1200 carriers are used. Accordingly, also in case of full use of the DSS resources, there are some unused REs in the frames. Indeed, only a fraction of such REs is related to the different number of 4G and 5G subcarriers, while the remaining ones are intrinsic in the 4G as well as 5G subframe structures. The exact number of unused REs in case of full 4G/5G traffic depends on how the scheduler allocates the 4G and 5G data in the DSS frame. This is a decision of the provider, and the almost 50 % sharing of the

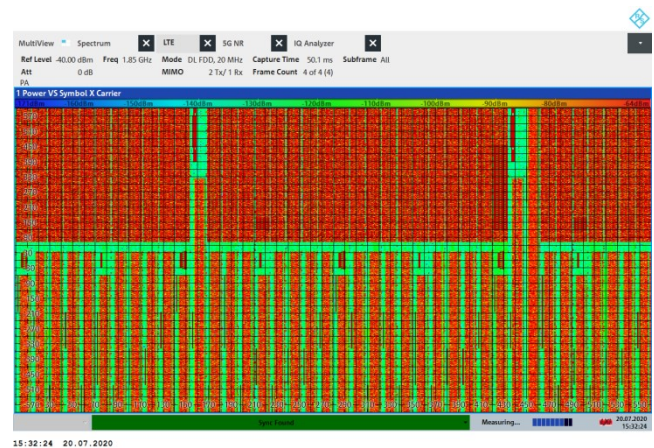


Figure 9. Power vs. symbol \times Carrier map of a DSS frame in case of 4G/5G balanced traffic.

Table 2. RS and PBCH-DMRS power per RE.

P_{RS}	-69.94 dBm
$P_{PBCH-DMRS}$	-70.20 dBm

Table 3. Comparison of MPE and CP measurement.

4G MPE	-38.90 dBm
5G MPE	-39.15 dBm
CP	-41.24 dBm

frame between 4G and 5G signals in case of full 4G and 5G traffic shown in Figure 9 is just one possible choice. Different choices give a slightly different number of 'unused' REs in case of fully filled frames. Consequently, the hypothesis of full use of the REs of the DSS frame carried out in the MPE procedure gives a conservative estimation of the maximum power level in case of full 4G/5G traffic for any possible distribution of the 4G/5G data chosen by the providers, according to the precautionary principle applied to the evaluation of the electromagnetic exposure of the population.

To verify the above observations, we have applied Eq. (3) and (4) to the full-loaded DSS signal in Figure 9. The PRS and P_{PBCH_DMRS} have been measured in the code domain and are reported in Table 2. Then, a Channel Power measurement was performed on the same signal. The MPE and CP measurements are reported in Table 3.

Results show that the use of Eq. (3) and (4) gives very close values, and confirm the conservative value obtained using MPE compared to the Channel Power result.

5. CONCLUSIONS

The EMF human exposure to DSS signals is a topic which is gaining growing interest among scientific community. In this paper the results of a study regarding the use of 4G or 5G MPE procedures for DSS signal are reported and found in good agreement with those reported in [19]. The DSS signals were generated by a base station emulator and transferred to the measurement instruments through an air interface adapter to obtain a controlled environment. This allowed to focus the analysis on the effect of the frame structure on the MPE procedure, excluding the random effects associated to fading phenomena affecting signals received in real environments.

The analysis confirms that both the 4G and the proposed 5G MPE procedures can be used for MPE of DSS signals, provided that the correct number of subcarriers in the DSS frame is considered.

REFERENCES

- [1] IEC 62232. Determination of RF field strength, power density and SAR in the vicinity of radiocommunication base stations for the purpose of evaluating human exposure. IEC - International Electrotechnical Commission, 2017.
- [2] S Aerts, L. Verloock, M. Van Den Bossche, D. Colombi, L. Martens, C. Tornevik, W. Joseph, W. In-situ Measurement Methodology for the Assessment of 5G NR Massive MIMO Base Station Exposure at Sub-6 GHz Frequencies. IEEE Access 2019, 7, 184658–184667. DOI: [10.1109/ACCESS.2019.2961225](https://doi.org/10.1109/ACCESS.2019.2961225).
- [3] D. Franci, S. Coltellacci, E. Grillo, S. Pavoncello, T. Aureli, R. Cintoli, M. D. Migliore, Experimental Procedure for Fifth Generation (5G) Electromagnetic Field (EMF) Measurement and

Maximum Power Extrapolation for Human Exposure Assessment. Environments 2020, 7, 22. 294 DOI: [10.3390/environments7030022](https://doi.org/10.3390/environments7030022)

- [4] D. Franci, S. Coltellacci, E. Grillo, S. Pavoncello, T. Aureli, R. Cintoli, M. D. Migliore, An Experimental Investigation on the Impact of Duplexing and Beamforming Techniques in Field Measurements of 5G Signals. Electronics 2020, 9, 223. DOI: [10.3390/electronics9020223](https://doi.org/10.3390/electronics9020223)
- [5] S. Adda, T. Aureli, S. D'Elia, D. Franci, E. Grillo, M. D. Migliore, S. Pavoncello, F. Schettino, R. Suman, A Theoretical and Experimental Investigation on the Measurement of the Electromagnetic Field Level Radiated by 5G Base Stations. IEEE Access 2020, 8, 101448–101463. 301 DOI: [10.1109/ACCESS.2020.2998448](https://doi.org/10.1109/ACCESS.2020.2998448)
- [6] M. D. Migliore, D. Franci, S. Pavoncello, E. Grillo, T. Aureli, S. Adda, R. Suman, S. D'Elia, F. Schettino, A New Paradigm in 5G Maximum Power Extrapolation for Human Exposure Assessment: Forcing gNB Traffic Toward the Measurement Equipment. IEEE Access 2021, 9, 101946–101958. DOI: [10.1109/ACCESS.2021.3092704](https://doi.org/10.1109/ACCESS.2021.3092704).
- [7] P. Baracca, A. Weber, T. Wild, C. Grangeat, A statistical approach for RF exposure compliance boundary assessment in massive MIMO systems, WSA 2018 - 22nd International ITGWorkshop on Smart Antennas, Bochum, Germany, 14-16 March 2018.
- [8] K. Bechta, C. Grangeat, J. Du, Impact of Effective Antenna Pattern on Radio Frequency Exposure Evaluation for 5G Base Station with Directional Antennas. 2020 XXXIII General Assembly and Scientific Symposium of the International Union of Radio Science. IEEE, 2018, pp. 1–4.
- [9] B. Thors, A. Furuskar, D. Colombi, C. Tornevik, Time-Averaged Realistic Maximum Power Levels for the Assessment of Radio Frequency Exposure for 5G Radio Base Stations Using Massive MIMO. IEEE Access 2017, 5, 19711–19719. DOI: [10.1109/ACCESS.2017.2753459](https://doi.org/10.1109/ACCESS.2017.2753459).
- [10] D. Pinchera, M. Migliore, F. Schettino, Compliance Boundaries of 5G Massive MIMO Radio Base Stations: A Statistical Approach. IEEE Access 2020, 8, 182787–182800. DOI: [10.1109/ACCESS.2020.3028471](https://doi.org/10.1109/ACCESS.2020.3028471).
- [11] D. Colombi, P. Joshi, B. Xu, F. Ghasemifard, V. Narasaraju, C. Törnevik, Analysis of the Actual Power and EMF Exposure from Base Stations in a Commercial 5G Network. Appl. Sci. 2020, 10, 5280. DOI: [10.3390/app10155280](https://doi.org/10.3390/app10155280).
- [12] S. Aerts, L. Verloock, M. Van den Bossche, D. Colombi, L. Martens, C. Tornevik, W. Joseph, Design and validation of an in-situ measurement procedure for 5G NR base station RF-EMF exposure. Joint Annual Meeting of the Bioelectromagnetics Society and the European BioElectromagnetics Association (BioEM 2020), 2020, pp. 414–418.
- [13] C. Bornkessel, T. Kopacz, A. M. Schiffarth, D. Heberling, M. A. Hein, Determination of Instantaneous and Maximal Human Exposure to 5G Massive-MIMO Base Stations. 2021 15th European Conference on Antennas and Propagation (EuCAP). IEEE, 2021, pp. 1–5.
- [14] M. D. Migliore, F. Schettino, Power Reduction Estimation of 5G Active Antenna Systems for Human Exposure Assessment in Realistic Scenarios. IEEE Access 2020, 8, 220095–220107. 331 DOI: [10.1109/ACCESS.2020.3042002](https://doi.org/10.1109/ACCESS.2020.3042002).
- [15] A. Hirata, Y. Diao, T. Onishi, K. Sasaki, S. Ahn, D. Colombi, V. De Santis, I. Laakso, L. Giaccione, W. Joseph, et al. Assessment of human exposure to electromagnetic fields: Review and future directions. IEEE Transactions on Electromagnetic Compatibility 2021.
- [16] M. D. Migliore, D. Franci, S. Pavoncello, E. Grillo, T. Aureli, S. Adda, R. Suman, S. D'Elia, F. Schettino, A New Paradigm in 5G Maximum Power Extrapolation for Human Exposure Assessment: Forcing gNB Traffic Toward the Measurement Equipment. IEEE Access 2021, 9, 101946–101958. DOI: [10.1109/ACCESS.2021.3092704](https://doi.org/10.1109/ACCESS.2021.3092704).

- [17] D. Franci, S. Coltellacci, E. Grillo, S. Pavoncello, T. Aureli, R. Cintoli, M.D. Migliore, Experimental Procedure for Fifth Generation (5G) Electromagnetic Field (EMF) Measurement and Maximum Power Extrapolation for Human Exposure Assessment. *Environments* 2020, 7, 342.
DOI: [10.3390/environments7030022](https://doi.org/10.3390/environments7030022)
- [18] TS 36.213. Evolved Universal Terrestrial Radio Access (E-UTRA); Physical layer procedures. 3rd Generation Partnership Project (3GPP), 2015
- [19] L. M. Schilling, C. Bornkessel, M. A. Hein, Analysis of Instantaneous and Maximal RF Exposure in 4G/5G Networks With Dynamic Spectrum Sharing, 16th European Conference on Antennas and Propagation (EuCAP), 2022, pp. 1-5.
DOI: [10.23919/EuCAP53622.2022.9769680](https://doi.org/10.23919/EuCAP53622.2022.9769680).